Supporting Information

Stability, Structure, Dynamics and Thermal Properties of C-type Aluminiumtrisdihydrogenphosphate

Sheyi C. Adediwura[a], Jan K. Wied[a], Christian F. Litterscheid[b], Jörn Schmedt auf der Günne*[a]

[a]University of Siegen, Faculty IV: School of Science and Technology, Department for Chemistry and Biology, Inorganic Materials Chemistry and Center of Micro- and Nanochemistry and (Bio)Technology (Cμ), Adolf-Reichwein Straße 2, 57076 Siegen, Germany.

[b]Chemische Fabrik Budenheim KG, Rheinstrasse 27, 55257 Budenheim, Germany.

*E-mail: gunnej@chemie.uni-siegen.de

Table of Contents

S1 Bulk Modulus of $Al(H_2PO_4)_3$ Polymorphs

The third-order Birch–Murnaghan isothermal equation of state is given by:[1]

$$P=\frac{3}{2}B_0\left[\left(\frac{V_0}{V}\right)^{7/3}-\left(\frac{V_0}{V}\right)^{5/3}\right]\cdot\left(1+\frac{3}{4}(B_0'-4)\left[\left(\frac{V_0}{V}\right)^{2/3}-1\right]\right) \qquad (1)$$

Table S1: Bulk modulus B_0, pressure derivative of bulk modulus B_0' and reference volume V_0 of $Al(H_2PO_4)_3$ polymorphs obtained using third-order Birch–Murnaghan isothermal equation of state.

Compounds	B_0 / GPa	B_0'	V_0 /Å³
A-type $Al(H_2PO_4)_3$	69.57	3.23	470.41
B-type $Al(H_2PO_4)_3$	37.88	4.76	453.79
C-type $Al(H_2PO_4)_3$	21.67	5.08	515.37

In comparison, the bulk modulus B_0 of KH_2PO_4 is 21.17 GPa.[2]

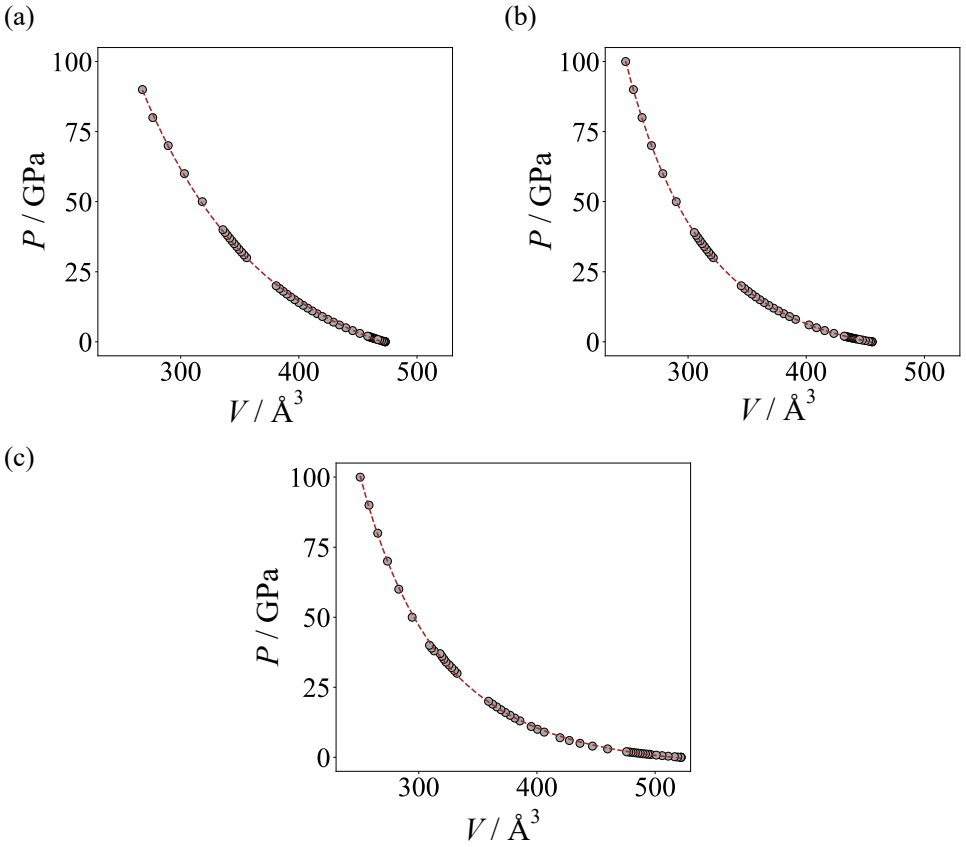

Figure S1: The plot of applied pressure p versus the resulting unit cell volume V for (a) A-type $Al(H_2PO_4)_3$ (b) B-type $Al(H_2PO_4)_3$, and (c) C-type $Al(H_2PO_4)_3$, obtained through density functional theory (DFT) calculations with variable-cell relaxation under different cell pressures (grey circles). The data was also modelled using the third-order Birch–Murnaghan isothermal equation of state (brown dashed line) as given in Equation 1, to obtain the bulk modulus B_0.

S2 Solid-state NMR Characterisation

S2.1 C-type $Al(H_2PO_4)_3$ with H_3PO_4

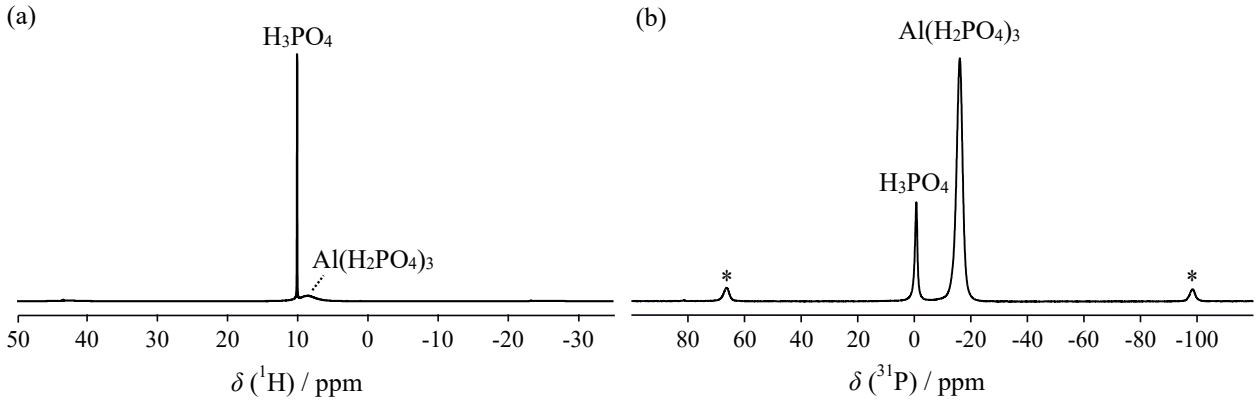

Figure S2: (a) ^{1}H, and (b) ^{31}P MAS NMR spectra of C-type $Al(H_2PO_4)_3$ showing H_3PO_4 impurity, obtained with a sample spinning frequency at 20 kHz, respectively. The asterisk (*) represents spinning side bands.

S2.2 Phase-pure C-type $Al(H_2PO_4)_3$

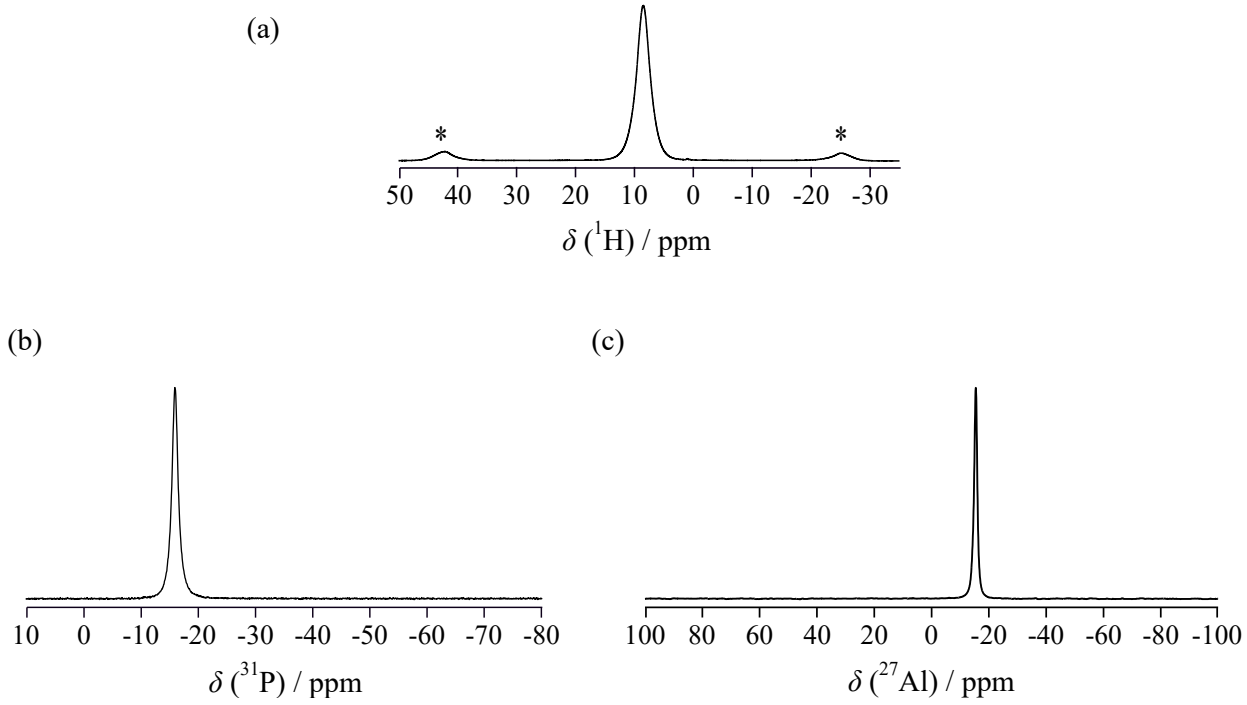

Figure S3: ^{1}H, ^{31}P, and ^{27}Al MAS NMR spectra of C-type $Al(H_2PO_4)_3$ obtained with a sample spinning frequency at 20 kHz, respectively. The asterisk (*) represents spinning side bands.

S2.3 Experimental and Fitted ^{31}P and ^{27}Al MAS NMR Spectra of C-type $Al(H_2PO_4)_3$

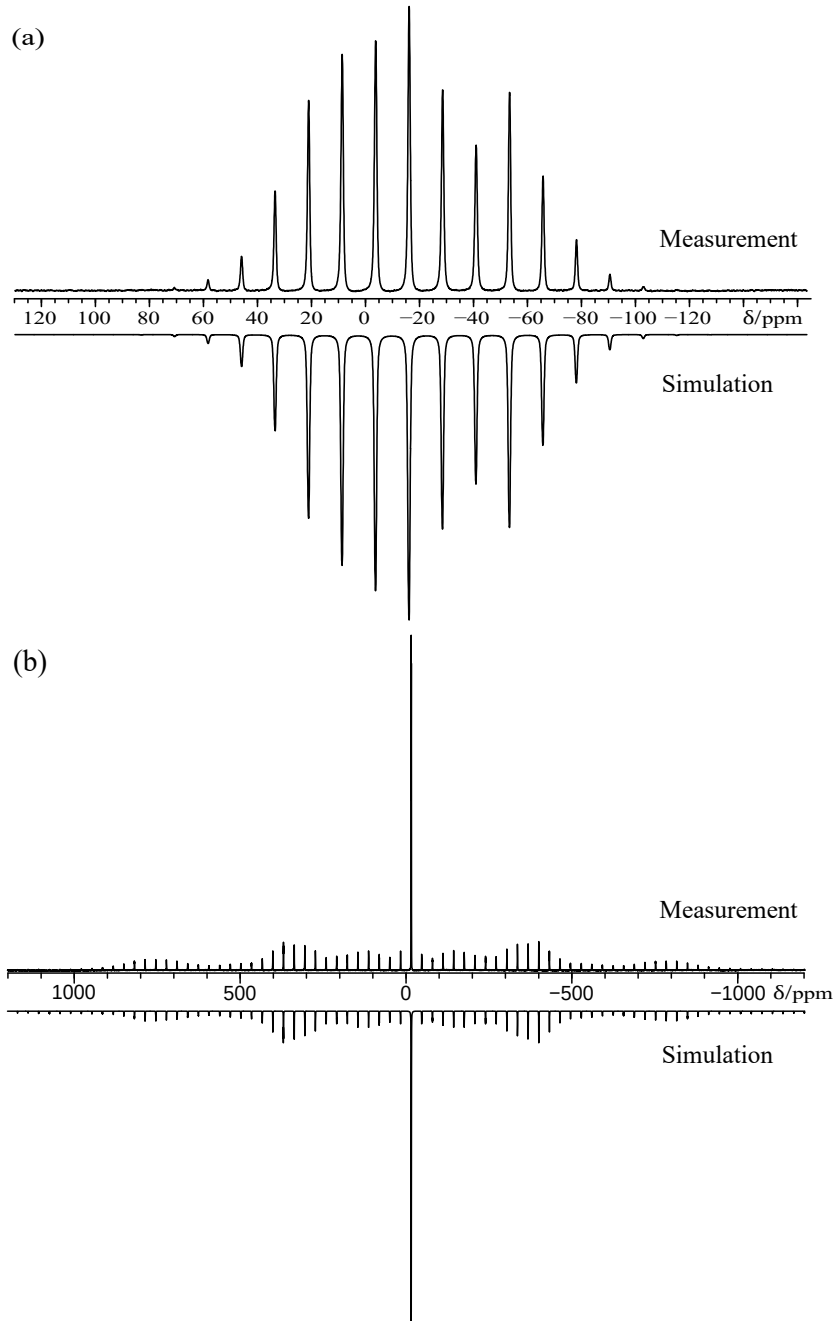

Figure S4: Experimental and simulated (a) ^{31}P (b) ^{27}Al MAS NMR spectrum of C-type $Al(H_2PO_4)_3$ were obtained with a sample spinning frequency of 4 and 6 kHz for ^{31}P and ^{27}Al MAS NMR, respectively. The chemical shift parameters were determined by non-linear least squares fitting (see Tables S1 and S2 for the resultant chemical shift values).

S2.4 Experimental and Fitted ^{31}P and ^{27}Al MAS NMR Spectra of $Al_2(P_6O_{18})$

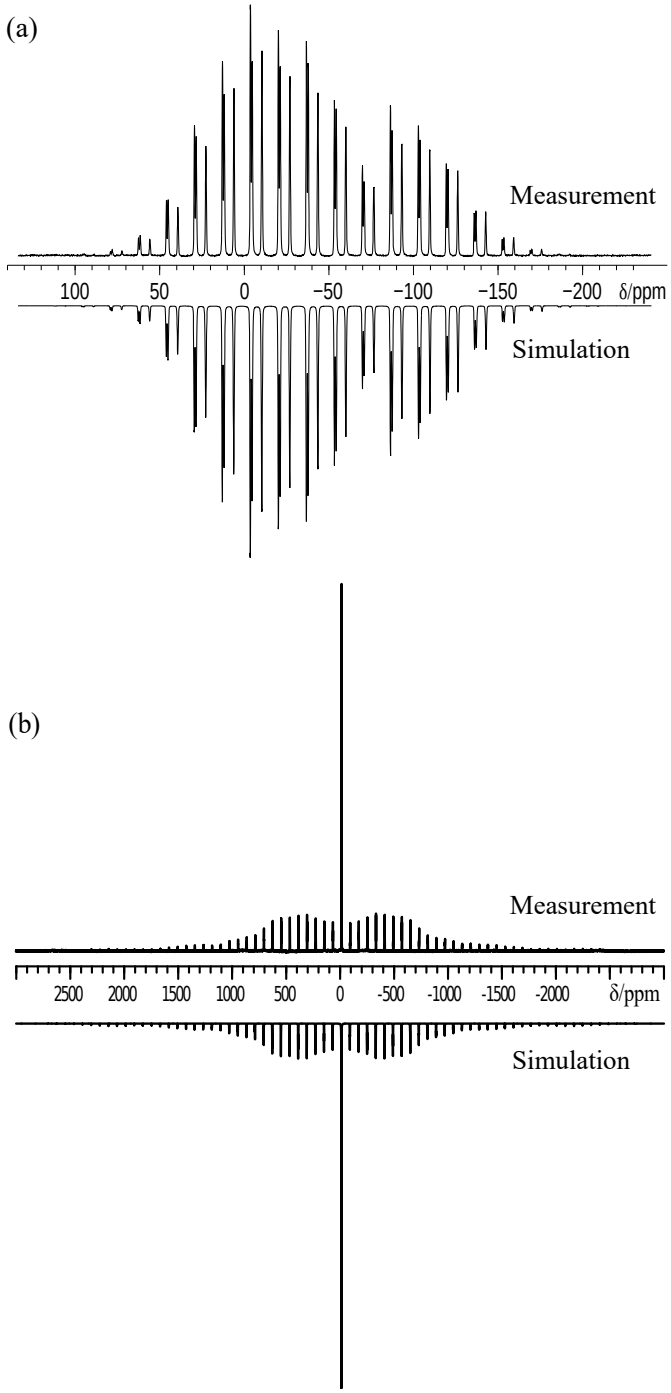

Figure S5: Experimental and simulated (a) ^{31}P (b) ^{27}Al MAS NMR spectrum of $Al_2(P_6O_{18})$ were obtained with a sample spinning frequency of 4 and 6 kHz for ^{31}P and ^{27}Al MAS NMR, respectively. The chemical shift parameters were determined by non-linear least squares fitting (see Tables S1 and S2 for the resultant chemical shift values).

S2.5 Experimental and Fitted ^{31}P and ^{27}Al MAS NMR Spectra of $Al_4(P_4O_{12})_3$

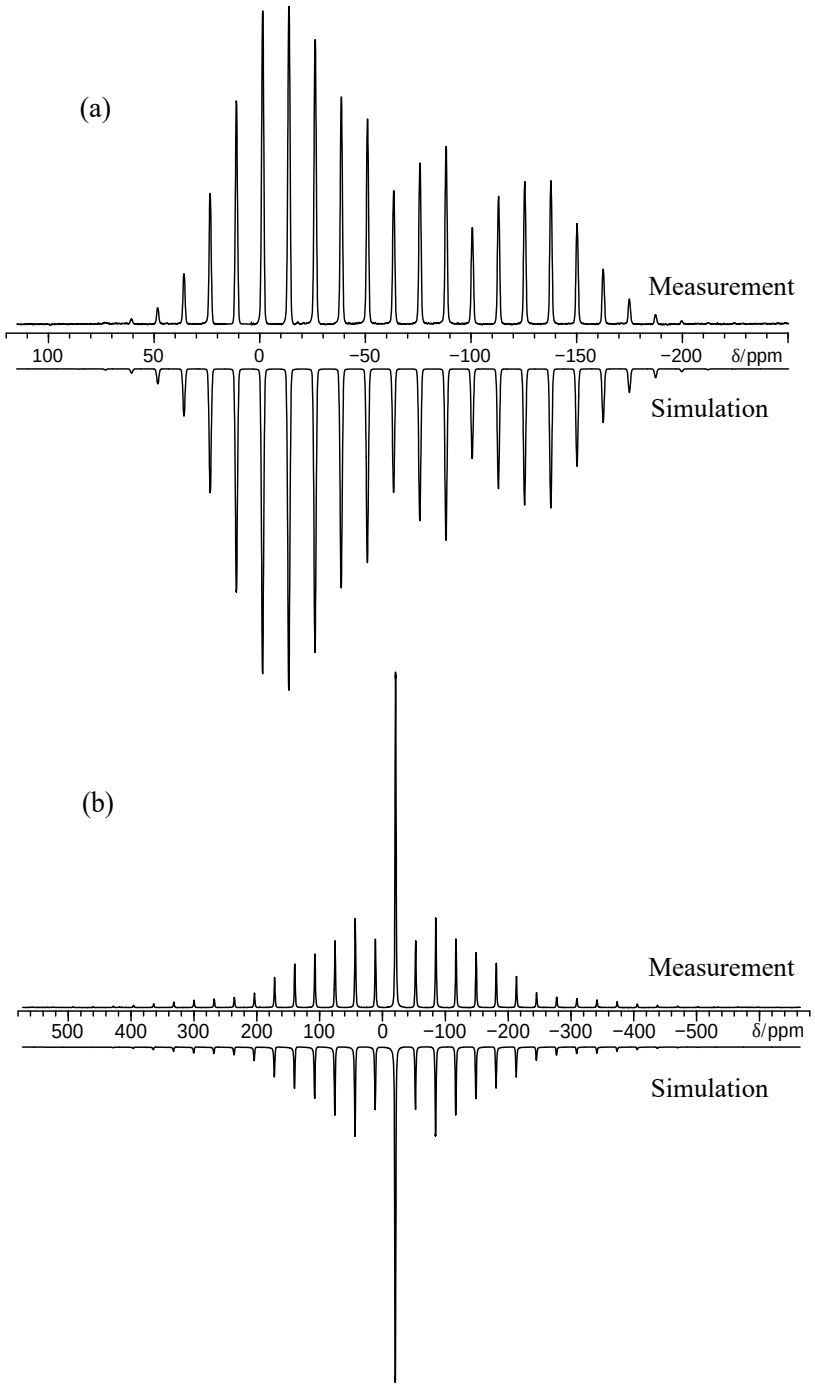

Figure S6: Experimental and simulated (a) ^{31}P (b) ^{27}Al MAS NMR spectrum of $Al_4(P_4O_{12})_3$ were obtained with a sample spinning frequency of 4 and 6 kHz for ^{31}P and ^{27}Al MAS NMR, respectively. The chemical shift parameters were determined by non-linear least squares fitting (see Tables S1 and S2 for the resultant chemical shift values).

S3 Pawley Refinement Analysis of C-type $Al(H_2PO_4)_3$

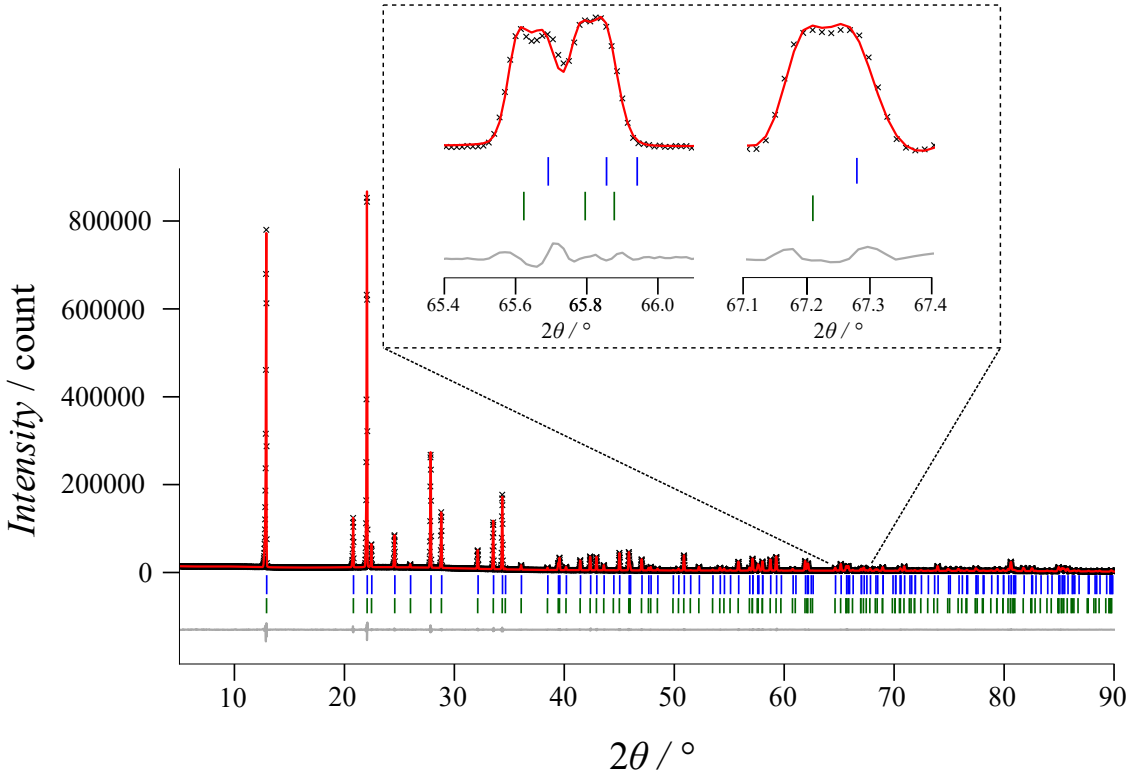

Figure S7: Pawley refinement of X-ray diffraction data of C-type $Al(H_2PO_4)_3$ obtained with Cu $K\alpha_1$ radiation (λ = 1.54056 Å) in Debye–Scherrer geometry. The experimental data (black x), the refined fit (red line), and the difference profile (grey line) are presented, along with the expected C-type Bragg reflections (blue line) and C'-type Bragg reflections (green line). The refinement yields weighted profile *R*-factor R_{wp} of 2.7 %, profile *R*-factor R_p of 2 %.

S4 Proton Conductivity Studies of C-type $Al(H_2PO_4)_3$

S4.1 Electrochemical Impedance Spectroscopy of C-type $Al(H_2PO_4)_3$

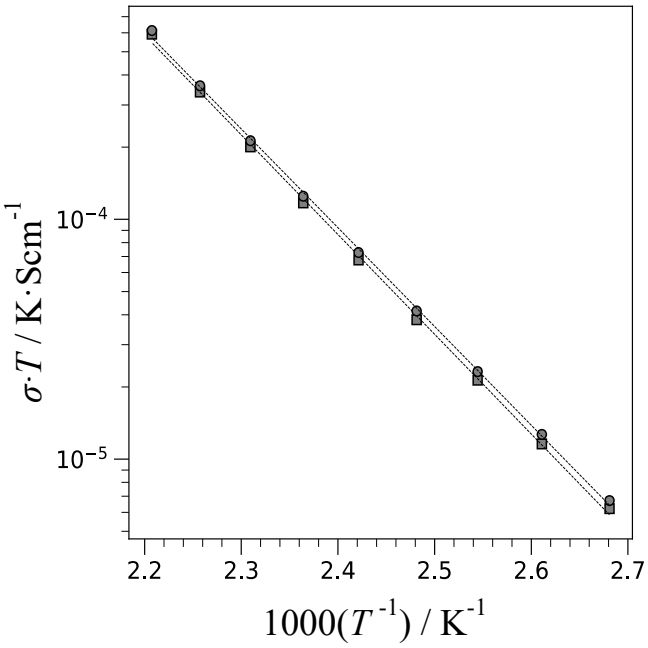

Figure S8: Plot of the product of electrical conductivity σ and temperature T versus inverse temperature for C-type $Al(H_2PO_4)_3$. The results were obtained from impedance spectra in temperature range from 373 K to 453 K. Linear fits are indicated by dashed lines. The data points are indicated by grey square and circle markers of the bulk conductivities for heating and cooling cycles, respectively.

Table S2: The macroscopic conductivity of C-type $Al(H_2PO_4)_3$ at 373 K and 453 K, pre-exponential factor a_0 and the activation energy E_a for heating and cooling cycles.

	Heating cycle	**Cooling cycle**
$\sigma_{373\,K}$ / (S· cm^{-1})	1.51(4) ·10^{-8}	1.68(4) ·10^{-8}
$\sigma_{453\,K}$ / (S· cm^{-1})	1.20(3) ·10^{-6}	1.23(3) ·10^{-6}
a_0 / (S· K· cm^{-1})	727836(1)	558168(1)
E_a / eV	0.82(1)	0.81(1)

S4.2 C-type $Al(H_2PO_4)_3$ Line Shape Analysis from ^1H NMR

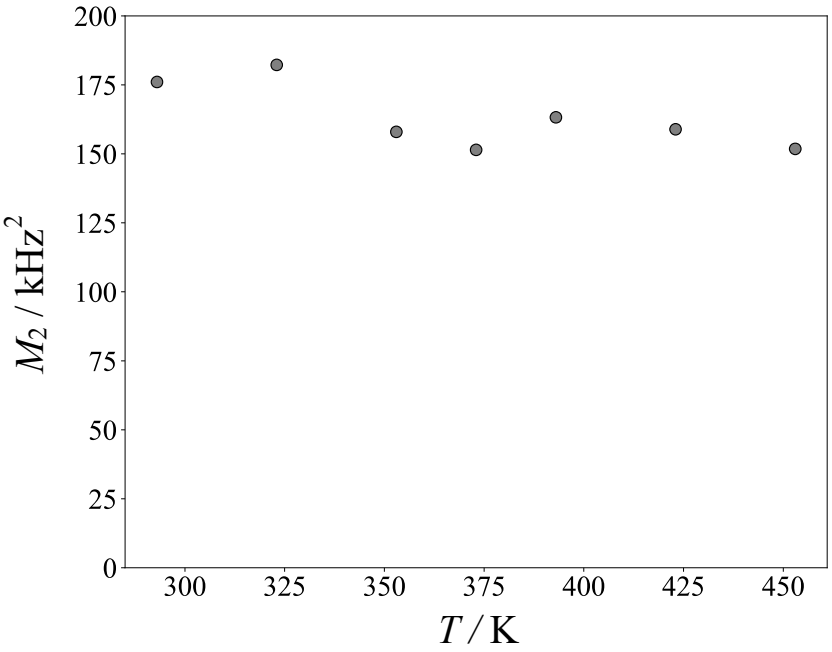

Figure S9: The second moment M_2 of C-type $Al(H_2PO_4)_3$ at different temperatures calculated from its ^1H NMR spectra of static powder samples measured at a frequency of 600 MHz.

S5 Powder Diffractograms of $Al_2(P_6O_{18})$

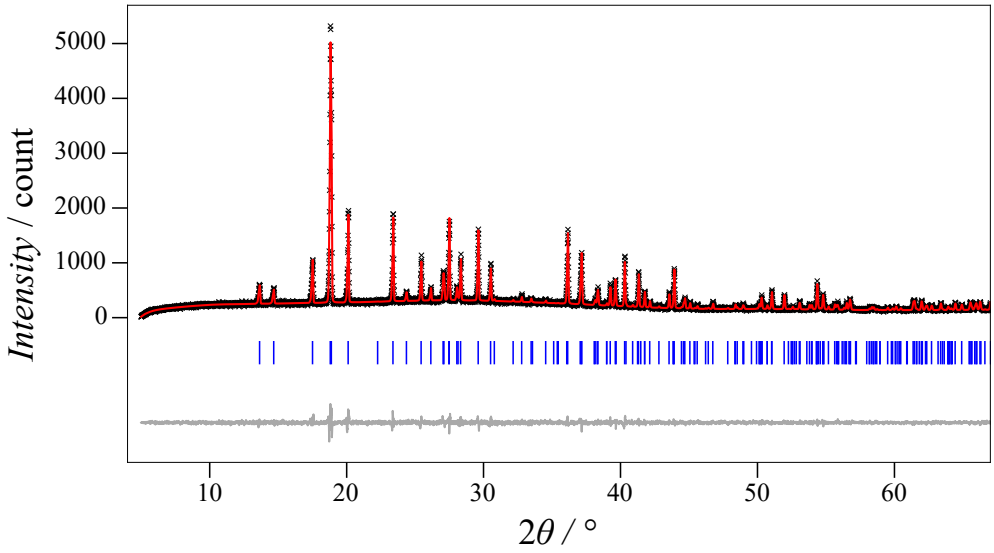

Figure S10: Observed (black x marker) powder diffraction pattern of $Al_2(P_6O_{18})$ measured with Co $K\alpha_1$ radiation (λ=1.78896 Å) and calculated diffraction pattern (red lines) using the Rietveld refinement. The grey line represents the difference profile, while the vertical blue lines are Bragg positions of $Al_2(P_6O_{18})$ (ICSD-260723).

S6 ^{31}P 2D Double-quantum MAS NMR of $Al_2(P_6O_{18})$

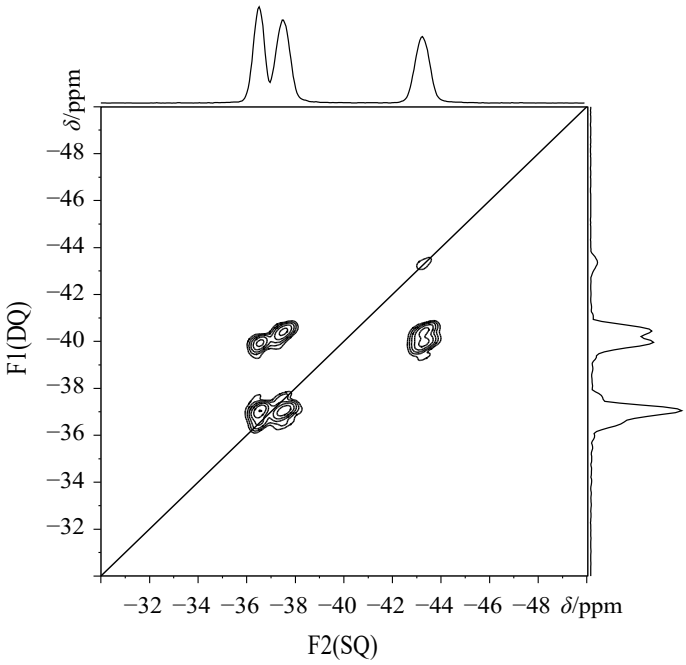

Figure S11: The ^{31}P-^{31}P 2D double-quantum NMR spectrum of $Al_2(P_6O_{18})$, acquired at a spinning frequency of 20 kHz, clearly identifies the connectivity of the three phosphorus sites through the intense cross-peak observed in the double-quantum dimension. The indirect scale is scaled such that DQ signals of isochronous pairs are on the diagonal.

S7 Rietveld Refinement Analysis of $Al_4(P_4O_{12})_3$

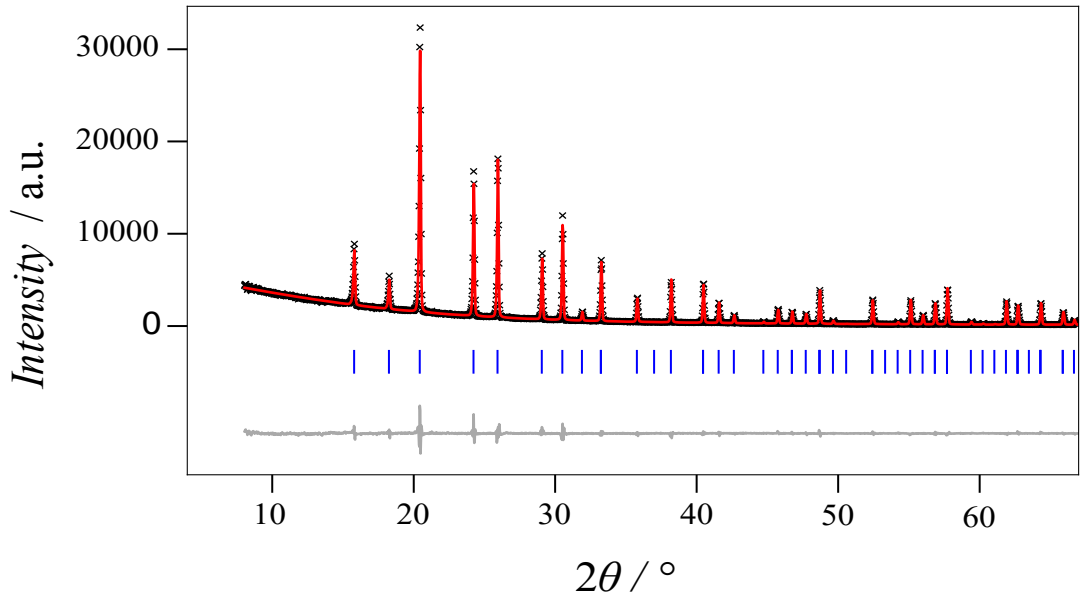

Figure S12: Rietveld refinement of $Al_4(P_4O_{12})_3$ X-ray diffraction pattern obtained with Cu $K\alpha_1$ radiation (λ = 1.54056 Å) in asymmetric transmission geometry. The experimental data (black x marker), the refined fit (red line), and the difference profile (grey line) are presented, along with the expected Bragg reflections (blue line). The refinement yields a weighted profile *R*-factor R_{wp} of 5.8 % and profile *R*-factor R_p of 4.3 %.

Table S3: Crystallographic data (atomic coordinates *x*, *y*, *z*, Anisotropic displacement parameters B_{eq} and occupancy) of $Al_4(P_4O_{12})_3$ at room temperature, obtained from Rietveld refinements of X-ray powder data (λ = 1.54056 Å) and space group $I\bar{4}3d(220)$

			Previous structural model		**Refined structural model**	
Crystal system			cubic		cubic	
a / Å			13.63[3]		13.735(2)	
Space group			$I\bar{4}3d(220)$		$I\bar{4}3d(220)$	
Z			4		4	
Atom	**Wyckoff site**	***x***	***y***	***z***	**Occ.**	B_{eq} /Å²
Al1	16*c*	0.1063(2)	0.1063(2)	0.1063(2)	1	0.77(10)
P1	48*e*	0.1197(1)	0.3316(2)	0.0469(2)	1	0.64(5)
O1	48*e*	0.1498(3)	0.2315(3)	0.0768(3)	1	0.61(6)
O2	48*e*	0.0179(3)	0.3611(3)	0.0597(3)	1	0.61(6)
O3	48*e*	0.1871(4)	0.4085(3)	0.1002(3)	1	0.61(6)

S8 Comparison of $Al_4(P_4O_{12})_3$ XRD Powder Patterns

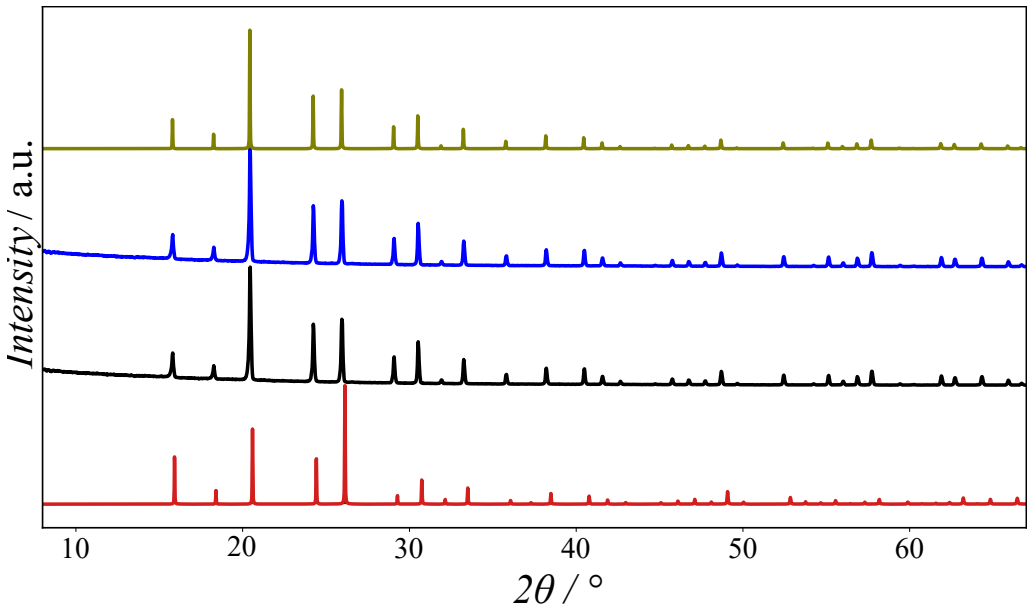

Figure S13: Powder diffractograms of $Al_4(P_4O_{12})_3$, obtained using transmission geometry with Cu $K\alpha_1$ radiations. The stack plot shows; the diffractogram of earlier published structure from 1937 (ICSD-26759) showing unsatisfactory match of the intensities(red), the experimental diffractogram (black), the best fit from Rietveld refinement (navy), and the simulated diffractogram from quantum-chemical relaxation calculations using Quantum Espresso (olive).

S9 Exemplary Rietveld Refinement Input File

S9.1 C-Type $Al(H_2PO_4)_3$ Rietveld Refinement

Table S4: Exemplary Rietveld refinement input file (used in Topas academic package[4]) with the refined parameters for C-type $Al(H_2PO_4)_3$ powder diffraction (Figure 2) recorded in Debye–Scherrer geometry.

r_wp 5.19927733
r_p 3.27342967
r_exp 0.884991911
gof 5.87494333
iters 500000
chi2_convergence_criteria 0.0001
do_errors
xdd S04636_180s_1.2d_05point_3runs_merged.xy

start_X 0

finish_X 65.5

bkg @ 8407.15533`_12.747238 -5494.1094`_22.5802597 821.037559`_21.2204504 826.695002`_20.6114756 -65.1104509`_19.9661207 -563.444101`_19.7429994 94.1112431`_19.1057072 505.23969`_18.8507229 -395.021654`_18.3756846 -73.9619347`_18.2363054 305.316224`_17.6748619 -124.026685`_17.5827333

-84.3168139`_17.0313804 52.16089`_16.9376807 -22.6569221`_16.1229988 15.051854`_15.7836736 14.6548318`_13.9783252 -61.6190222`_13.5302062

convolution_step 5

---

lam

ymin_on_ymax 0.0001

la 1 lo 1.540596 lh 0.501844

Radius(180)

LP_Factor(!lp,27.28)

Zero_Error(zero,-0.0175035992`_0.000473531142)

Divergence(div, 0.557081668`_0.0155287783)

prm varx 0.136058608`_0.00216891728 min 0.001 max 0.99

Slit_Width(varx)

Simple_Axial_Model(axial, 8.00928425`_0.0132123506)

---

str

phase_name "C-type Al(H2PO4)3"

a lpa 13.686208`_0.000121

b =lpa;

c lpb 9.133267`_0.000102

al 90.000000

be 90.000000

ga 120.000000

volume 1489.316951

space_group "R3c"

site P1 x @ 0.00331`_0.00031 y @ 0.16229`_0.00018 z @ 0.26559`_0.00086 occ P 1.0 beq UP 1.23636`_0.04729

site AL1 x 0.000000 y 0.000000 z 0.000000 occ Al 1.0 beq UAl 0.61344`_0.08080

site O1 x x1 0.03397`_0.00047 y y1 0.12706`_0.00051 z z1 0.39982`_0.00091 occ O 1.0 beq UO 0.82853`_0.04626

site O2 x x2 0.58107`_0.00031 y y2 0.53538`_0.00033 z z2 0.62043`_0.00089 occ O 1.0 beq = UO;

site O3 x x3 0.45122`_0.00032 y y3 0.50449`_0.00030 z z3 0.37841`_0.00078 occ O 1.0 beq = UO;

```
site O4    x x4  0.12515`_0.00051 y y4  0.03071`_0.00051 z z4  0.12560`_0.00094 occ O    1.0        beq = UO;

site H1     x = x2 + ph1*(x3 - x2);
            y = y2 + ph1*(y3 - y2);
            z = z2 + ph1*(z3 - z2);      occ H    1.0      beq = 1.5*UO;

site H2     x = 1.0-y3 + ph2*(-1.0+y3 + x2);
            y = 1.0-x3 + ph2*(-1.0+x3 + y2);
            z = z3+0.5 + ph2*(-z3-0.5 + z2);      occ H    1.0      beq = 1.5*UO;

    prm !ph1  0.650
    prm !ph2  0.644

scale @  0.00206553187`_6.448e-06
r_bragg  3.03292577
TCHZ_Peak_Type(!pku,0,pkv,  0.0125424394`_0.00116424413,pkw, -0.00165993766`_0.000152072331,!pkz, 0.0000,!pky, 0,!pkx, 0.0000)

Phase_Density_g_on_cm3( 2.13809604`_4.48691129e-05)

CS_L(size_lor, 5830.52487`_491.987944_LIMIT_MAX_8531.90852)
Strain_G(strain_g, 0.12447234`_0.0059024573)
Phase_LAC_1_on_cm( 70.8787413`_0.00148742909)
phase_MAC @  33.150401
cell_volume @  1481.573`_0.031
Cell_mass @  1907.660
```

S9.2 $Al_4(P_4O_{12})_3$ Rietveld Refinement

Table S5: Exemplary Rietveld refinement input file (used in TOPAS academic software package [4]) with the refined parameters for $Al_4(P_4O_{12})_3$ powder diffraction (Figure S12).

```
r_wp      5.80514732
r_exp     3.1888741
r_p       4.27780404
gof       3.1888741

do_errors

xdd s04651.xy
```

x_calculation_step = Yobs_dx_at(Xo);

convolution_step 5

start_X 0

finish_X 90

bkg @ 1027.03662`_1.69431554 -1523.43685`_3.07444168 970.113295`_2.80245604 -463.59384`_2.63746407 166.42279`_2.49320327 -33.4265054`_2.24378176 -15.102972`_2.05488934 15.2501819`_1.5501455 -3.16635192`_1.20318802

convolution_step 5

LP_Factor(!th2_monochromator, 27.28)

CuKa1(0.0001)

Zero_Error(@ , 0.0732308178`_0.0560759589)

Specimen_Displacement(height, 0.0130547927`_0.0254913276)

Divergence(@, 0.878269378`_0.0940954403)

Full_Axial_Model(12, 15, 12, 2.3, @ 6.09483`_0.06436)

Tube_Tails(, 0.00487350562,, -0.0388314018,, 0.00329872058_LIMIT_MIN_1e-05,, 0.0620669557)

Rp 220

Rs 57.3

---

str

phase_name " Al4(P4O12)3 "

Cubic(@ 13.734941`_0.002345)

volume 2598.30506

space_group "I-43d"

site Al1 x lx 0.10633`_0.00015 y = lx; z = lx; occ Al 1 beq bAl 0.76819`_0.09699

site P1 x @ 0.11974`_0.00012 y @ 0.33162`_0.00020 z @ 0.04688`_0.00020 occ P 1 beq bP 0.63594`_0.05298

site O1 x @ 0.14977`_0.00031 y @ 0.23147`_0.00033 z @ 0.07679`_0.00025 occ O 1 beq Bo 0.60834`_0.06023

site O2 x @ 0.01792`_0.00031 y @ 0.36112`_0.00027 z @ 0.05969`_0.00034 occ O 1 beq =bO;

site O3 x @ 0.18708`_0.00040 y @ 0.40854`_0.00031 z @ 0.10024`_0.00026 occ O 1 beq =bO;

---

scale @ 4.14845664e-05`_2.314e-07

r_bragg 1.77941187

CS_G(size_gau, 114.627085`_2.21696305)

Phase_Density_g_on_cm3(2.70597717`_0.00138546788)

PO_Spherical_Harmonics(sh, 8 load sh_Cij_prm {

k00 !sh_c00 1.00000

k41 sh_c41 0.01232`_0.00731

k61 sh_c61 0.02836`_0.00963

k81 sh_c81 -0.01093`_0.00844

}

TCHZ_Peak_Type(pku, 0.00587141453`_0.00189276075,pkv, 0.00356126169`_0.00122084622,pkw, -0.00110446235`_0.000227120448,!pkz, 0.0000,pky, 0.0001`_0.00462695425_LIMIT_MIN_0.0001,pkx, 0.0208973281`_0.00173070466)

Phase_LAC_1_on_cm(102.401871`_0.0524300442)

phase_MAC @ 37.8428436

cell_volume @ 2591.077`_1.327

cell_mass @ 4222.359

References

[1] F. Birch, *Phys. Rev.* **1947**, *71*, 809–824.
[2] S. Yang, L. Zhang, *Ceram. Int.* **2021**, *47*, 15875–15882.
[3] L. Pauling, J. Sherman, *Z. Kristallogr. - Cryst. Mater.* **1937**, *96*, 481–487.
[4] A. A. Coelho, *J. Appl. Cryst.* **2018**, *51*, 210–218.